*Mineralogical Magazine* (2019), **83**, 381–392
doi:10.1180/mgm.2018.164

CAMBRIDGE UNIVERSITY PRESS

**Article**

# Subaerial sulfate mineral formation related to acid aerosols at the Zhenzhu Spring, Tengchong, China

Lianchao Luo[1,2], Huaguo Wen[1,2]*, Rongcai Zheng[1,2], Ran Liu[2], Yi Li[2], Xiaotong Luo[2] and Yaxian You[2]

[1]State Key Laboratory of Oil and Gas Reservoir Geology and Exploitation (Chengdu University of Technology), Chengdu 610059, China; and [2]Institute of Sedimentary Geology, Chengdu University of Technology, Chengdu 610059, China

**Abstract**

The Zhenzhu Spring, located in the Tengchong volcanic field, Yunnan, China, is an acid hot spring with high $SO_4^{2-}$ concentrations and intense acid aerosol generation. In order to understand the formation mechanism of sulfate minerals at the Zhenzhu Spring and provide a better insight into the sulfur isotope geochemistry of the associated Rehai hydrothermal system, we investigated the spring water hydrochemistry, mineralogy and major-element geochemistry of sulfate minerals at the Zhenzhu Spring together with the sulfur-oxygen isotope geochemistry of sulfur-containing materials at the Rehai geothermal field and compared the isotope results with those in other steam-heated environments. Subaerial minerals include a wide variety of sulfate minerals (gypsum, alunogen, pickeringite, tamarugite, magnesiovoltaite and a minor Mg–S–O phase) and amorphous $SiO_2$. The $\delta^{34}S$ values of the subaerial sulfate minerals at the Zhenzhu Spring varied subtly from −0.33 to 1.88‰ and were almost consistent with the $\delta^{34}S$ values of local $H_2S$ (−2.6 to 0.6‰) and dissolved $SO_4^{2-}$ (−0.2 to 5.8‰), while the $\delta^{18}O$ values (−8.94 to 20.1‰) were between that of the spring waters (−10.19 to −6.7‰) and atmospheric $O_2$ (~23.88‰). The results suggest that most of the sulfate minerals are derived from the oxidation of $H_2S$, similar to many sulfate minerals from modern steam-heated environments. However, the rapid environmental change (different ratio of atmospheric and water oxygen) at the Zhenzhu Spring accounts for the large variation of $\delta^{18}O$. The formation of subaerial sulfate minerals around the Zhenzhu Spring is related to acid aerosols (vapour and acid water droplets). The intense activity of spring water around vents supply the aerosol with $H_2SO_4$ ($H_2S$ oxidation and acid water droplets formed by bubble bursting) and few cations. Deposition of the acid sulfate aerosol forms the acid condensate, which attacks the underlying rocks and releases many cations and anions to form subaerial sulfate minerals at the Zhenzhu Spring.

**Keywords:** Tengchong, subaerial environment, sulfate mineral, acid aerosol

(Received 24 April 2018; accepted 28 September 2018; Accepted Manuscript online: 14 January 2019; Associate Editor: G. Diego Gatta)

## Introduction

Sulfate minerals are common products associated with volcanism and geothermal activity throughout the world and include hydrous sulfate minerals (e.g. gypsum and alunogen) and anhydrous sulfate minerals (e.g. anhydrite and baryte). Such minerals have been found in various terrestrial environments, including fumaroles (Africano and Bernard, 2000; Hynek *et al.*, 2013; Adams *et al.*, 2017), active crater lakes (Pierre and Alain, 1994; Rodríguez and van Bergen, 2017), hot springs (Bonny and Jones, 2003; Sakae *et al.*, 2011; Tang *et al.*, 2014), caves in geothermal or volcanic settings (Rodgers *et al.*, 2000; White, 2010), and other environments with no volcanism or geothermal activities (Fernández-Remolar *et al.*, 2005; Stracher *et al.*, 2005; Valente and Gomes, 2009). Apart from some sulfate minerals precipitated from aqueous solutions (superficial water bodies), most of these minerals in volcanic and/or geothermal environments are ordinarily present as fumarolic encrustations, volcanic sublimates and efflorescences (Stoiber and Rose, 1974; Zhu *et al.*, 1980; Ciesielczuk *et al.*, 2013; Piochi *et al.*, 2015; Rodríguez and van Bergen, 2016). Unlike sulfate minerals deposited in seas or lakes, the formation mechanisms of these sulfate minerals are not solely confined to the evaporation of water under ambient conditions. Alteration of rocks by gas condensate on volcanoes is considered to be the primary formation mechanism (Kodosky and Keskinen, 1990; Africano and Bernard, 2000; McCollom *et al.*, 2013). In addition, several other less common formation mechanisms of volcanic/fumarolic sulfate minerals have also been proposed, such as capillary action with subsequent evaporation of pore water, deposition of vapours around volcanic vents, precipitation from thermal spring water, and acid-fog deposition around active volcanoes (Delines, 1975; Martin *et al.*, 1999; Bonny and Jones, 2003; Schiffman *et al.*, 2006).

At the Zhenzhu Spring (also known as Pearl Spring or Zhenzhuquan), located in Tengchong, Yunnan Province, southwestern China (Fig. 1), abundant sulfate deposits have formed around the spring (Fig. 1*d*), which are located in a subaerial, acid and humid environment. The acid aerosols (fog/steam), derived from pool water, are copious and appear to be related to the formation of the sulfate minerals. However, the mineralogical and chemical features, and the genesis of these minerals, remain unclear. Previous investigations of the Zhenzhu Spring have only focused on the spring water and gas geochemistry

*Author for correspondence: Huaguo Wen, Email: wenhuaguo08@cdut.cn
**Cite this article:** Luo L., Wen H., Zheng R., Liu R., Li Y., Luo X. and You Y. (2019) Subaerial sulfate mineral formation related to acid aerosols at the Zhenzhu Spring, Tengchong, China. *Mineralogical Magazine* **83**, 381–392. https://doi.org/10.1180/mgm.2018.164

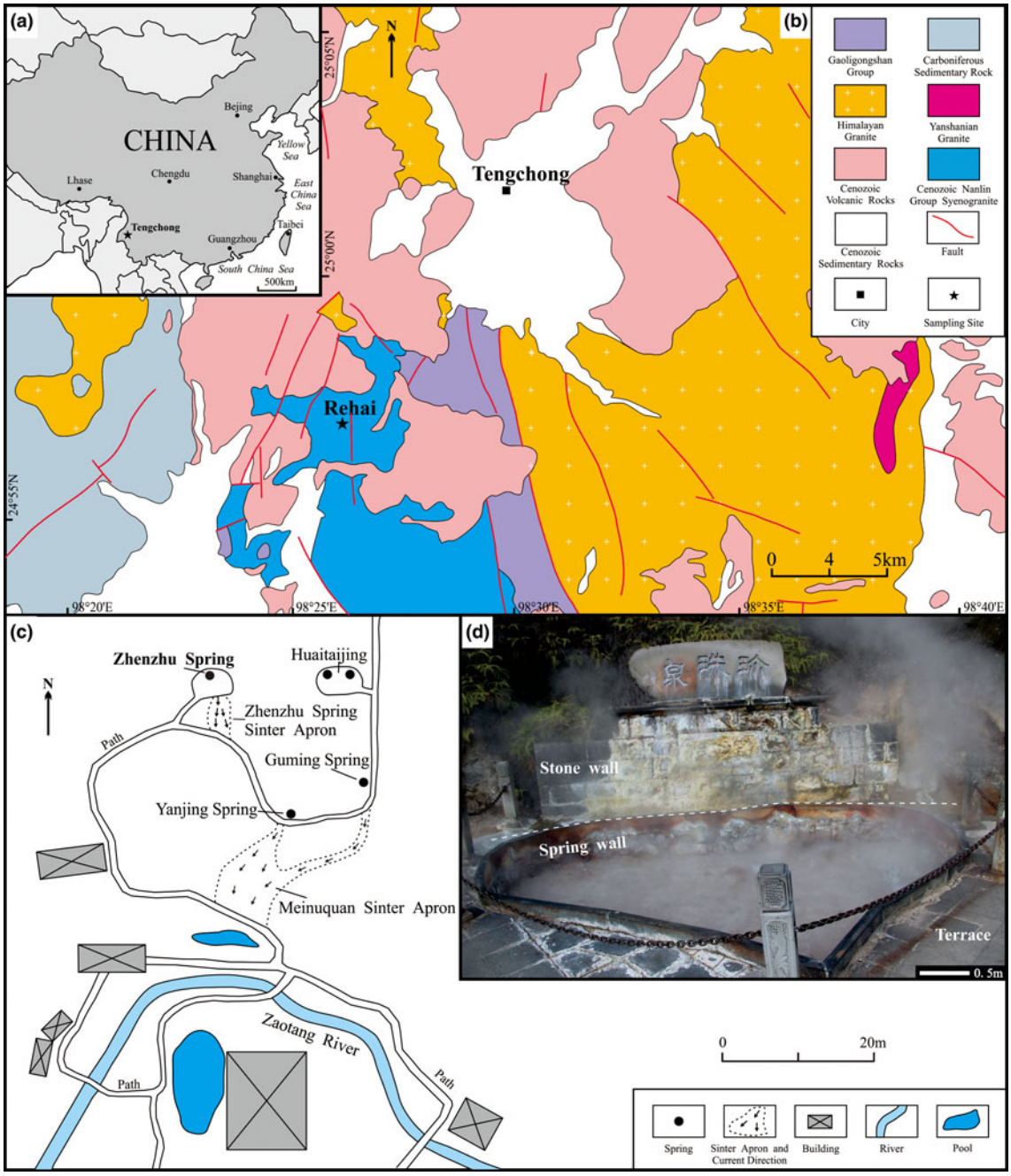


**Fig. 1.** Location of the Zhenzhu Spring. (*a*) Location of Tengchong in western Yunnan, southwest China. (*b*) Geological map of the area around the Rehai geothermal field where the Zhenzhu Spring is located, showing the distribution of granitic rocks in the Rehai geothermal field. (*c*) Map of the Zhenzhu Spring in the Rehai geothermal field, showing the locations of the Zhenzhu Spring and adjacent springs and sinter deposits. (*d*) General view of the heart-shaped Zhenzhu Spring showing the spring wall that surrounds the vent pool and the stone wall near the pool.

(e.g. Shangguan and Huo, 2002; Zhang *et al.*, 2008; Guo *et al.*, 2014), and microbiology (e.g. Hou *et al.*, 2013; Briggs *et al.*, 2014; Liu *et al.*, 2016). This investigation mainly focuses on the sulfate minerals in contact areas of acid aerosol and rock. Using samples collected from the Zhenzhu Spring, this research: (1) investigates the spring water hydrochemistry; (2) describes the distribution, mineralogical composition, crystal morphology, major-element geochemistry and sulfur-oxygen isotope signatures of subaerial minerals; and (3) compares the sulfur-oxygen composition of sulfate minerals from the Zhenzhu Spring with those from the Rehai geothermal field and other modern steam-heated environments. By combining this information, this investigation provides valuable insights into the formation mechanism of sulfate minerals at the Zhenzhu Spring and the sulfur-oxygen isotope geochemistry of the Rehai hydrothermal system.

## *General setting*

The Tengchong volcanic and geothermal field lies to the southeast of the Tibetan Plateau, in the western Yunnan Province, China (Fig. 1*a*). Sixty eight volcanoes exist in Tengchong (Zou *et al.*, 2010). The volcanoes developed along the Gaoligong dextral

https://doi.org/10.1180/mgm.2018.164 Published online by Cambridge University Press

strike-slip fault and near its intersection with the Ruili-Mandalay sinistral strike-slip fault (Huang *et al.*, 2013). There are three famous volcanoes in Tengchong: Dayingshan; Maanshan; and Heikongshan. The volcanic zone is quite active; the latest eruption of Maanshan volcano, the youngest volcano, took place only ~3800 years ago (Jiang, 1998). Tengchong has a wide distribution of volcanic rocks with an outcrop of up to 1000 $km^2$ (Fig. 1*b*), including basalt, basaltic andesite, dacite and andesite (Jiang *et al.*, 2018). Tengchong has a highland subtropical climate and can be broadly divided into two seasons: the dry season from October to April and the wet season extending from May to September (Jones and Peng, 2015). Temperature, rainfall and sunshine variations are apparent between the dry season (generally 8 to 18°C, 0 to 150 mm/month, 170 to 270 hours/month, respectively) and the wet season (generally 18 to 22, 140 to 340 mm/month, 70 to 180 hours/month, respectively) in Tengchong.

The Rehai geothermal field, located ~11 km southwest of Tengchong city (Fig. 1*b*), has an area of ~10 $km^2$. A large number of springs, with water temperatures varying from 42 to 96°C (Guo, 2012), occur at the Rehai geothermal field, distributed mainly in the valley of Zaotanghe River (Zhang *et al.*, 2008). Previous research (e.g. Hong *et al.*, 2009; Guo *et al.*, 2014) shows that most of the springs have near-neutral to alkaline waters. Only a few springs produce acidic water (pH < 4), including the Zhenzhu, Diretiyanqu and Laogunguo Springs. Furthermore, other evidence of geothermal activity has been found, including hydrothermal explosions, fumaroles, steaming ground, sinters, travertines and hydrothermal alteration. One magma chamber with a temperature of >400°C, is located below the Rehai geothermal field (Zhao *et al.*, 2011). This magma chamber is proven by the existence of areas of low-velocity anomalies and high conductivity in deep seismic sounding profiles (e.g. Wang and Gang, 2004; Xu *et al.*, 2012; Yang *et al.*, 2013). It is located 7 km below the surface and has a thickness up to 20 km (e.g. Bai *et al.*, 1994; Bai *et al.*, 2001; Jiang *et al.*, 2012). Residual heat from the magma chamber heats the groundwater, creating a hydrothermal convective system which forms hot or warm springs on the surface. The temperatures of the geothermal reservoirs, which are composed of Proterozoic metamorphic rocks and Yanshanian granitic rocks (Guo and Wang, 2012), vary between 60 and 450°C, but are mainly in the range 160 to 260°C (Liao *et al.*, 1991; Shangguan, 2000; Du *et al.*, 2005). The geothermal water from hot springs at the Rehai geothermal field is essentially derived from meteoric water (Du *et al.*, 2005).

## Methods

Detailed field observations, descriptions, photography and measurements of water parameters (*T*, pH) were taken in June 2016 and January 2017. Water samples were filtered through a 0.45 μm nylon membrane and collected in 500 ml polyethylene bottles which had been pre-washed with deionised water. A condenser was used to collect 50 ml of condensed steam. This apparatus has been employed by Hynek *et al.* (2013) to collect gas condensates from fumaroles. After sampling, the water samples were promptly sent for cation and anion analysis. A Thermo Corporation IRIS Intrepid II XSP ICP-OES was used to analyse major cations (Na, K, Ca, Mg, Fe and Al) and $SiO_2$ concentrations. Carbonate and bicarbonate concentrations were determined by titration with $HNO_3$ (0.1 M), described in Alcicek *et al.* (2016). The anions, including $Cl^-$ and $SO_4^{2-}$, were measured using ion chromatography (Dionex Thermo Corporation ICS 1100). The precision of the analyses is < 5% (RSD) for cations and $SiO_2$, and < 10% (RSD) for $Cl^-$ and $SO_4^{2-}$.

Scanning electron microscope (SEM) analyses and energy-dispersive X-ray (EDX) analyses were used to identify micromorphology and elemental compositions, respectively. Small solid samples (≤ 1 cm) were extracted and mounted on SEM stubs, after being bonded with conductive glue and coated with a thin gold layer. Three-dimensional images were produced by a QUANTA 250 FEG-scanning electron microscope at 5 kV, while EDX analyses were done with an accelerating voltage of 20 kV using an Oxford INCAx-max20 X-ray spectrometer. The average EDX spot size used was ~1 μm. Numerous EDX analyses were carried out to distinguish the minerals and precisely verify their composition. These analyses were conducted at the State Key Laboratory of Oil and Gas Reservoir Geology and Exploitation, Chengdu University of Technology.

X-ray diffraction (XRD) was used as the main method for mineral identification. Fourteen samples were chosen for XRD analysis utilising Cu*K*α radiation with a step size of 0.02° and 2θ range from 5 to 60° (DX-2700, Dandong Haoyuan), and was conducted at the College of Materials and Chemistry & Chemical Engineering, Chengdu University of Technology. Eleven samples were chipped and powdered into near 200 mesh size for major-element analysis. The powdered samples were then sent to the Institute of Multipurpose Utilization of Mineral Resources, Chinese Academy of Geological Sciences, and analysed using an X-ray fluorescence spectrometer (XRF, Axios max, Panalytical).

The $\delta^{34}S$ and $\delta^{18}O$ values were determined at the Beijing Createch Testing Technology Co., Ltd. Prior to sulfur and oxygen isotope analysis, the water samples were acidified to a pH of 3, heated to 80°C, mixed with 10% barium chloride solution to precipitate $BaSO_4$, washed repeatedly with distilled-deionised water and dried at 110°C. A dried $BaSO_4$ sample was obtained from sulfate minerals by the following protocols from Szynkiewicz *et al.* (2013): The solid samples (~5 g) were dried and ground using an agate mortar and pestle. The contribution of elemental S and sulfide was negligible because neither were observed in the XRD analyses. We directly treated the powder sample with 6 N HCl to dissolve the sulfate minerals and exclude the acid non-soluble substances (e.g. quartz, amorphous silica). NaOH was used to adjust the pH to 9–10, in order to remove dissolved iron by precipitation of iron oxides. Lastly, the same procedure for the extraction of dissolved $SO_4^{2-}$ in the water samples described above (acidifying, adding 10% barium chloride solution, and drying) was used to obtain $BaSO_4$. After the solid $BaSO_4$ was converted to $SO_2$ and CO, its $\delta^{34}S$ and $\delta^{18}O$ were measured with an Elemental Analyzer (EA) coupled with a Finnigan MAT 253 Plus (Thermo Fisher Scientific) ratio mass spectrometer. The analytical precision is estimated to be better than ± 0.2‰ ($\delta^{34}S$) and ± 0.5‰ ($\delta^{18}O$). The $\delta^{34}S$ and $\delta^{18}O$ were reported relative to the Vienna-Canyon Diablo Troilite (V-CDT) standard and the Vienna Standard Mean Ocean Water (V-SMOW), respectively.

## Results

### General description

Unlike most of the hot springs at the Rehai geothermal field, the Zhenzhu Spring is an acid sulfate spring with Na–$SO_4$–Cl-type waters formed by condensation and oxidation of $H_2S$-rich vapours in the shallow groundwater or surface water (Jiang

https://doi.org/10.1180/mgm.2018.164 Published online by Cambridge University Press

**Table 1.** Composition (mg/L) of spring water and condensed steam from the Zhenzhu Spring.

| Reference | Type | *T* (°C) | pH | $HCO_3$ | $SO_4^{2-}$ | Cl | Na | K | Ca | Mg | Fe | Al | $SiO_2$ | Charge balance error |
|---|---|---|---|---|---|---|---|---|---|---|---|---|---|---|
| Zhang *et al.* (2008) | Spring water | 96 | 3.5 | ND | 134 | 38.1 | 13 | 13.7 | 1.71 | 0.04 | 0.237 | | 153 | −48.70 |
| Guo and Wang (2012) | Spring water | 96 | 6.4 | 5.6 | 128.2 | 39.2 | 67.7 | 15.9 | 2.3 | 0.4 | | | 262 | −5.01 |
| Guo *et al.* (2014) | Spring water | 91.8 | 4.5 | 12.8 | 162 | 64.3 | 58.5 | 21.7 | 2.16 | 0.61 | 1.33 | | 140 | −23.26 |
| Jiang *et al.* (2018) | Spring water | 89.9 | 3.58 | 15.3 | 112.7 | 38.8 | 49 | 21.8 | 3.1 | 0.6 | 0.52 | 0.20 | | −7.05 |
| Jiang *et al.* (2018) | Spring water | 91.3 | 4.33 | 15.3 | 114.4 | 41.4 | 53.1 | 23.4 | 3.2 | 0.5 | 0.52 | 0.22 | | −8.47 |
| Jiang *et al.* (2018) | Spring water | 84.6 | 3.89 | 18.3 | 120.1 | 40.7 | 52 | 21.7 | 3.1 | 0.3 | 0.63 | 0.20 | | −10.78 |
| This research | Spring water | 92.2 | 3.63 | 20.7 | 120.8 | 41.26 | 62.34 | 22.93 | 2.02 | 0.53 | ND | 0.46 | 122.8 | −3.76 |
| This research | Spring water | 90.9 | 3.24 | 17.1 | 120.5 | 41.8 | 53.69 | 24.7 | 1.74 | 0.73 | 0.65 | 0.81 | 236.6 | −1.99 |
| This research | Condensed steam | 19.6* | 3.22* | ND | 34.0 | 0.107 | 0.267 | 0.183 | 5.11 | 0.185 | <0.03 | <0.1 | 0.295 | 11.10 |

ND = not detected, blank = no data. * = measured in the lab.

*et al.*, 2018). The Zhenzhu Spring has been artificially modified into a heart-shaped pool (Fig. 1*d*) with a depth of ~0.45 m and a maximum diameter of ~4.4 m. Characterised by a stable water depth thanks to a discharge channel, the Zhenzhu Spring has a water depth of ~8 cm. Numerous small vents are developed at the bottom. These vents release a large quantity of $CO_2$ gas ($CO_2$ = 94.5%) with very limited amounts of $N_2$, $O_2$, Ar, $H_2$, $CH_4$, He and $S_{total}$ ($S_{total}$ = 0.115%, including 0.101% $H_2S$ and 0.005% $SO_2$) (Shangguan *et al.*, 2000). The intense activity of the spring water results in the occurrence of aerosols above the Zhenzhu Spring. Colourful sulfate minerals cover the stone wall and the spring wall (Fig. 1*d*). During field observations, it was also noticed that Fe-staining (reddened rocks) occurs on the spring wall (Fig. 1*d*).

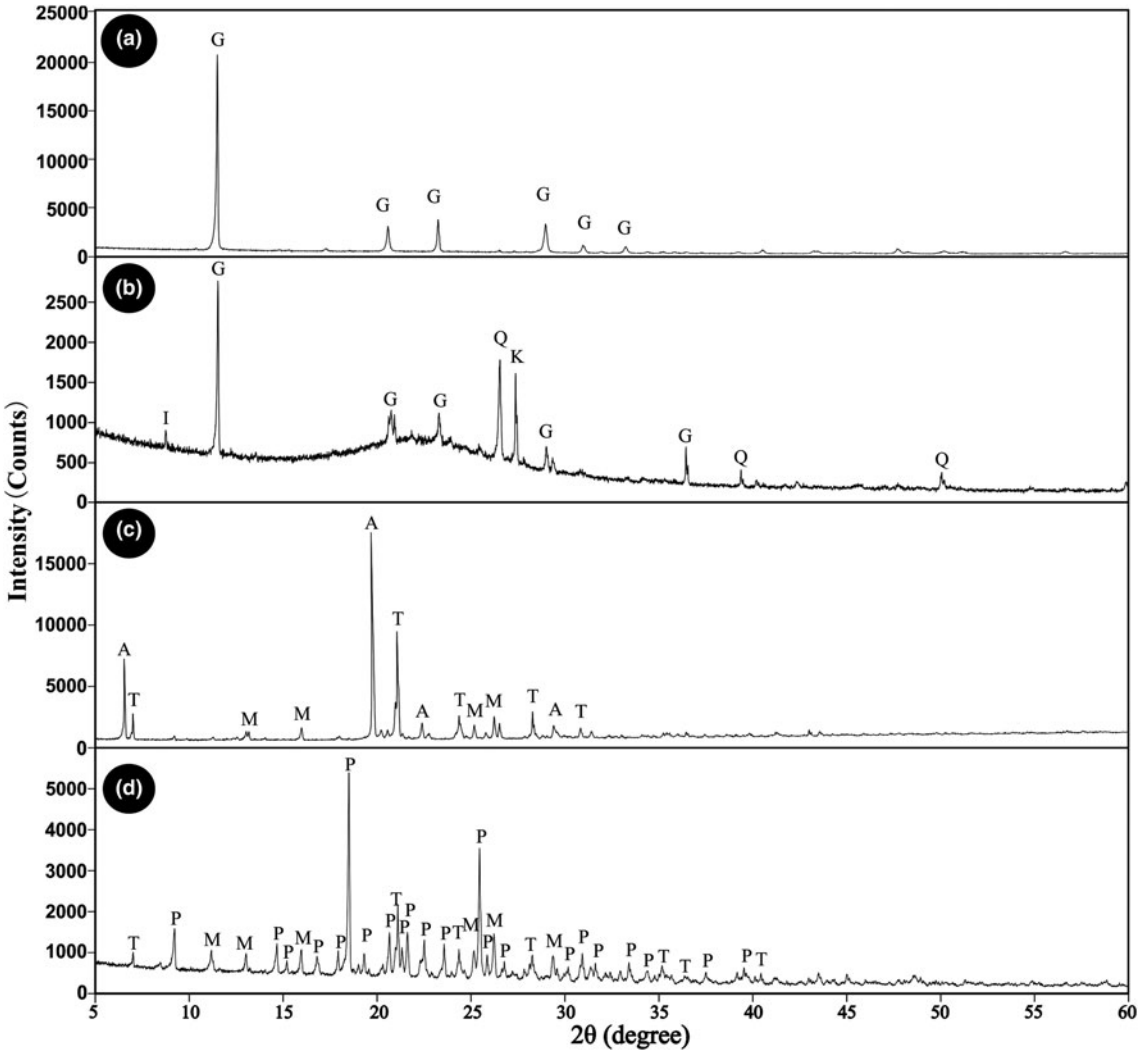


**Fig. 2.** XRD patterns for samples from the Zhenzhu Spring showing the presence of gypsum (G), amorphous $SiO_2$, quartz (Q), K-feldspar (K), illite (I), alunogen (A), tamarugite (T), magnesiovoltaite (M) and pickeringite (P).

https://doi.org/10.1180/mgm.2018.164 Published online by Cambridge University Press

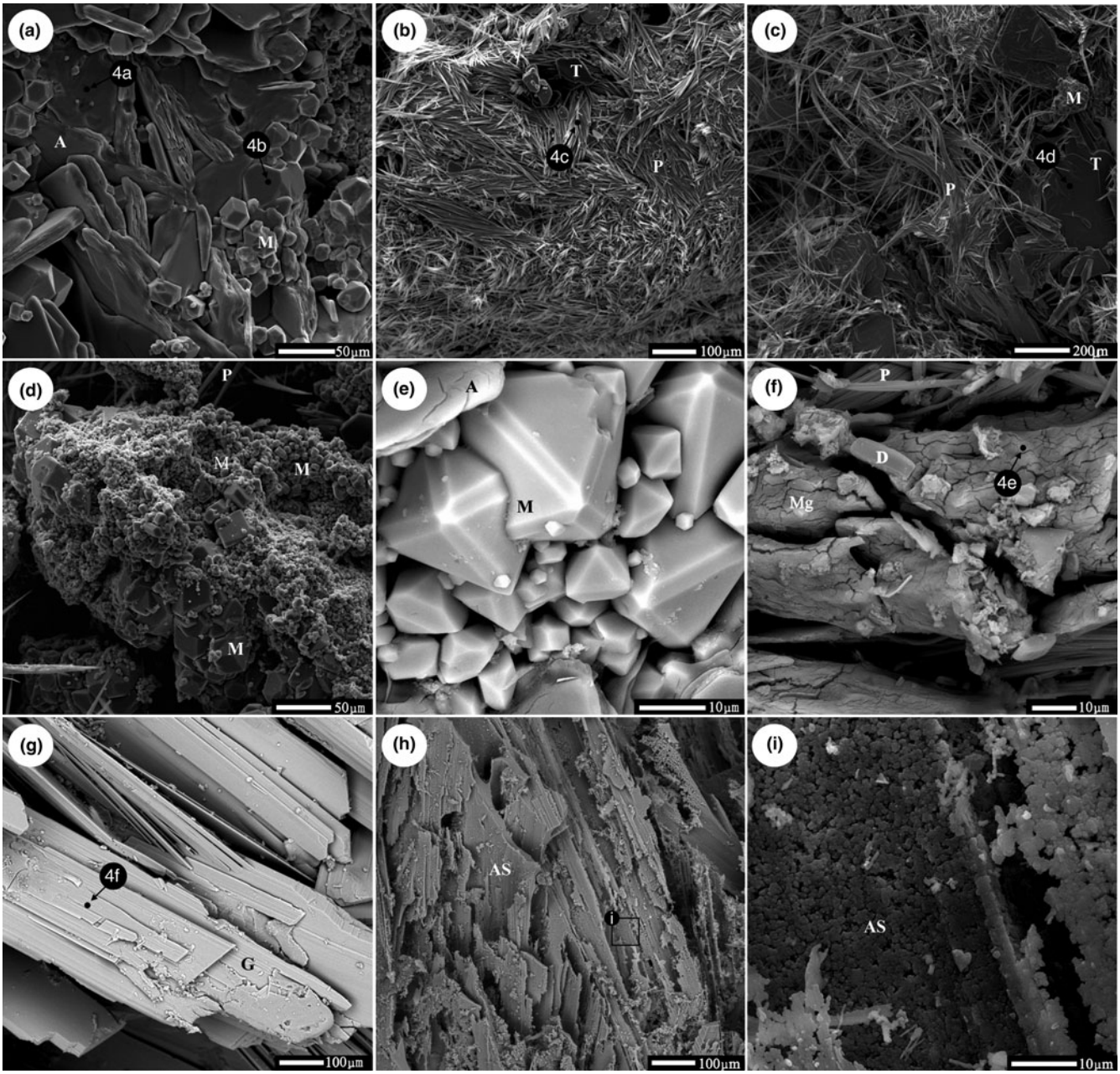


**Fig. 3.** Secondary electron (SE) and back-scattered electron (BSE) photographs of sulfate minerals (*a*–*g*) and amorphous $SiO_2$ (*h*, *i*). A = alunogen, M = magnesiovoltaite, T = tamarugite, P = pickeringite, Mg = Mg–S–O phase, G = gypsum, AS = amorphous $SiO_2$. Spot EDX analyses are in indicated in Fig. 4. (*a*) Tabular alunogen crystals and granular magnesiovoltaite crystals, SE. (*b*) Matted aggregate of pickeringite crystals with some tabular tamarugite crystals, SE. (*c*) Hair-like pickeringite crystals, tabular tamarugite crystals and aggregate of magnesiovoltaite crystals, SE. (*d*) Aggregates of magnesiovoltaite crystals of different sizes, SE. (*e*) Well-shaped magnesiovoltaite crystals, BSE. (*f*) Mg–S-O phase without distinct crystalline shapes and diatom (*d*), BSE. (*g*) Large thin tabular gypsum crystals which possess the same growing direction, BSE. (*h*) Tabular amorphous $SiO_2$ aggregates, BSE. Black box indicates the position of (*i*). (*i*) Tabular amorphous $SiO_2$ aggregates consisting of small amorphous $SiO_2$ particles, SE.

### *Chemistry of spring water and condensed steam*

The temperature, pH and major composition of fluids at the Zhenzhu Spring is given in Table 1. The spring waters are characterised by temperatures from 84.6 to 96°C and pH generally between 3.24 and 4.5. The waters predominately contain $SiO_2$, $SO_4^{2-}$, Na, Cl, K and $HCO_3$ (in decreasing order) and minor Ca, Mg, Fe and Al. Although the acidic condensed steam (pH = 3.22) mainly formed by aerosol precipitation, and vapour condensation from the Zhenzhu Spring shows lower ionic concentrations than the spring waters, the Ca concentration of this sample (>5 mg/L) is approximately three times the concentration of the spring waters (Table 1). The most abundant cation and anion in the condensed steam are $SO_4^{2-}$ and Ca, respectively. The remaining ions are present with <1 mg/L in the condensed steam. A significant difference in charge balance error values was found in different studies (Table 1). Although the reasons for this variation are not clear, it might be caused by laboratory analytical errors, different sampling procedures, unfiltered samples, etc.

https://doi.org/10.1180/mgm.2018.164 Published online by Cambridge University Press

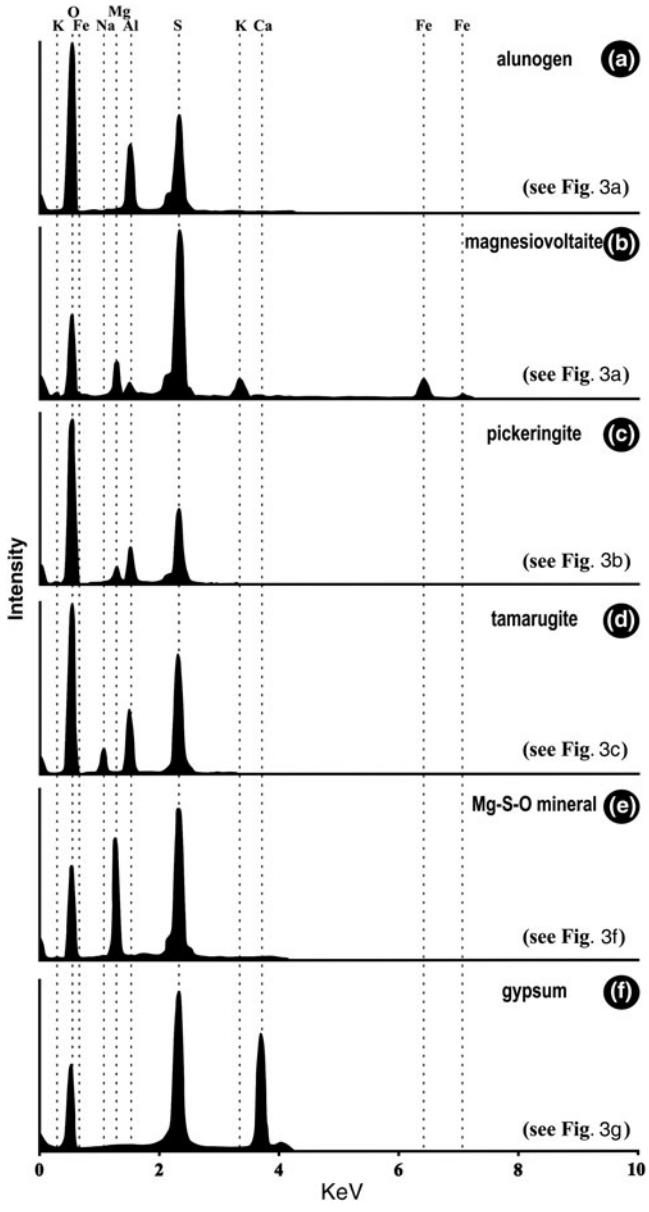


**Fig. 4.** EDX analyses of points shown in Fig. 3a, b, c, f and g, respectively.

### *Mineralogy*

Detailed XRD analyses and SEM-EDX analyses can be seen in Figs 2 to 4 and Table 2. The minerals in the samples can be divided into three groups: (1) sulfate minerals (alunogen, pickeringite, tamarugite, magnesiovoltaite, gypsum and an Mg–S–O phase); (2) silica minerals (amorphous $SiO_2$ and quartz); and (3) silicate minerals (K-feldspar and illite). Apart from the Mg–S–O phase, all the remaining minerals can be identified in XRD analyses (Fig. 2; Table 2). The quartz, K-feldspar and illite are derived mainly from the country rocks, which contain no metal-sulfide minerals, while the sulfate minerals and amorphous $SiO_2$ are the secondary minerals. There is a high content of amorphous $SiO_2$ in only one sample (Table 2). The amorphous $SiO_2$ shows a broad 'hump' with no apparent peaks in the XRD spectra (Fig. 2*b*) and occurs mainly as tabular aggregates (Fig. 3*h*, *i*).

Sulfate minerals were observed in all samples from the Zhenzhu Spring and covered a range of compositions (Table 2). Gypsum is abundant in most of the samples from the spring wall and generally appears with silicate minerals or amorphous $SiO_2$. SEM images show that the tabular gypsum crystals are common (Fig. 3*g*). Alunogen is also a major mineral, which has a tabular shape (Fig. 3*a*), and produces high O, S and Al X-ray peaks (Fig. 4*a*). Compared with the alunogen crystals, tamarugite, which occurs in lower concentrations, shows a smoother crystal surface and it is relatively thin in the microphotographs (Fig. 3*c*). Pickeringite, if present, is mainly developed as matted aggregates or hair-like crystals (Fig. 3*b*, 3*c*). Some of the samples contain an unusual mineral (magnesiovoltaite), which displays high Fe and K peaks in EDX analyses, in addition to O, Mg, Al and S X-ray peaks (Fig. 4*b*). This mineral generally exhibits a regular habit and appears as a mineral aggregate (Fig. 3*d*, *e*). Unlike other sulfate minerals from the samples, the Mg–S–O phase can only be found by SEM-EDX analyses and lacks normal geometric forms (Figs 3*f*, 4*e*). These Al-containing sulfate minerals (alunogen, tamarugite, etc.) were abundant in the samples from the stone wall (Fig. 1*d*).

### *Geochemistry*

Table 3 lists the major element compositions of sulfate samples from the Zhenzhu Spring. $SO_3$ contents are high and vary from 29.1 to 42.6 wt.%. Other components, ignoring $SO_3$ however, are variable and can be divided into two groups (Table 2). $SiO_2$ and CaO are the abundant components in Group 1, reflecting the enrichment of gypsum and amorphous $SiO_2$, while $Na_2O$, MgO, and $Al_2O_3$ are depleted. In contrast, $Na_2O$, MgO, $Al_2O_3$ and $Fe_2O_3$ (total contents varying from 18.0 to 21.0 wt.%) are enriched in Group 2 because of the presence of many hydrated Al-containing sulfate minerals. Also, many of the precipitates have high $H_2O$ contents, as partly indicated by high loss on ignition (LOI) values (up to 42.2 wt.%), which might reflect the presence of hydrated phases (hydrated sulfate minerals and/or amorphous $SiO_2$).

The results of the sulfur and oxygen isotope analyses of sulfate minerals, dissolved $SO_4^{2-}$, $H_2S$, sulfide and $O_2$ at the Zhenzhu Spring and other springs at the Rehai geothermal field, and in some typical steam-heated environments, are present in Table 4 and Fig. 5. Samples from the Zhenzhu Spring show a narrow range of $\delta^{34}S$ values (–0.33 to 1.8‰), which are close to the $\delta^{34}S$ values of $H_2S$ (–2.9 to 1.8‰) and dissolved $SO_4^{2-}$ (–0.2 to 5.8‰) at the Rehai geothermal field. Additionally, a large $\delta^{18}O$ range (–8.94 to 20.1‰) is observed, falling between the $\delta^{18}O$ values of dissolved $SO_4^{2-}$ at the Rehai geothermal field (–10.19 to –6.7‰) and those of atmospheric $O_2$ (~23.88‰ ± 0.02‰). The $\delta^{34}S$ range of the Al-containing sulfate minerals (–0.05 to 1.47‰) from the Zhenzhu Spring is similar to the range of the gypsum (–0.33 to 1.88‰). However, compared with the negative $\delta^{18}O$ values of the gypsum-containing samples (Population 1: –8.94 to –4.62‰) mainly occurring on the spring wall (approximating the spring water, Fig. 1*d*), the Al-containing minerals from the stone wall (Fig. 1*d*) have higher $\delta^{18}O$ values (Population 2: 6.71 to 8.93‰, Population 3: 16.48 to 20.1‰). The spring water from the Zhenzhu Spring contains sulfur and oxygen isotope compositions that are consistent with the solid samples enriched in gypsum.

## Discussion

### *Genesis of sulfate minerals*

Gas condensate alteration, which is usually considered to be a leading factor in the formation of sulfate minerals from fumaroles

https://doi.org/10.1180/mgm.2018.164 Published online by Cambridge University Press

**Table 2.** Minerals identified using X-ray diffraction.

| No. | Alunogen $Al_2(SO_4)_3{\cdot}17H_2O$ | Pickeringite $MgAl_2(SO_4)_4{\cdot}22H_2O$ | Tamarugite $NaAl_2(SO_4)_2{\cdot}6H_2O$ | Magnesiovoltaite $K_2Mg_5Fe^{3+}_3Al(SO_4)_{12}{\cdot}18H_2O$ | Gypsum $CaSO_4{\cdot}2H_2O$ | Amorphous $SiO_2$ $SiO_2{\cdot}nH_2O$ | Quartz $SiO_2$ | K-feldspar $KAlSi_3O_8$ | Illite $(K,H_3O)(Al,Mg,Fe)_2(Si,Al)_4O_{10}[(OH)_2,(H_2O)]$ |
|---|---|---|---|---|---|---|---|---|---|
| 1 | | | | | XXXX | | XX | | |
| 2 | | | | | XXXX | | | | |
| 3 | | | | | XXX | XXXX | XX | XX | X |
| 4 | | | | | XXXX | | XX | XX | |
| 5 | XXXX | XXX | | XX | | | | | |
| 6 | XXXX | XXX | | XX | | | | | |
| 7 | | XXXX | XXX | XX | | | | | |
| 8 | XXXX | | XX | X | | | | | |
| 9 | | | | | XXXX | | XX | X | |
| 10 | | | | | XXXX | | | | |
| 11 | | | | | XX | | XXXX | X | |
| 12 | | | | | XXXX | | X | | |
| 13 | | | | | XXXX | | | | |
| 14 | | | | | XXXX | | | | |

XXXX: content > 50%, XXX: 50% ≥content > 20%, XX: 20% ≥content > 5%, X: content ≤5%, Blank = no data

**Table 3.** Major element (wt.%) compositions as determined by X-ray fluorescence from the Zhenzhu Spring samples.

| Type | $Na_2O$ | MgO | $Al_2O_3$ | $SiO_2$ | $SO_3$ | $K_2O$ | CaO | $Fe_2O_3$ | LOI | Total |
|---|---|---|---|---|---|---|---|---|---|---|
| Group 1 | 0.09 | 0.05 | 0.93 | 27.43 | 31.14 | 0.87 | 19.69 | 3.21 | 17.15 | 100.55 |
| | ND | ND | 0.58 | 34.04 | 29.14 | 0.41 | 19.65 | 0.53 | 17.37 | 101.71 |
| | ND | 0.05 | 0.83 | 18.29 | 36.49 | 0.34 | 24.79 | 0.07 | 20.04 | 100.89 |
| | ND | ND | 0.34 | 15.00 | 38.18 | 0.16 | 26.66 | 0.03 | 20.51 | 100.87 |
| | ND | ND | 0.17 | 13.27 | 37.49 | 0.07 | 27.46 | 0.03 | 22.81 | 101.30 |
| | 0.13 | 0.30 | 1.32 | 10.36 | 36.83 | 0.35 | 26.03 | 0.31 | 25.08 | 100.71 |
| | 0.08 | 0.14 | 1.00 | 8.27 | 38.52 | 0.23 | 27.21 | 0.16 | 25.41 | 101.01 |
| Group 2 | 2.15 | 3.54 | 10.38 | 1.62 | 41.85 | 0.89 | 0.34 | 3.52 | 37.76 | 102.05 |
| | 1.07 | 5.00 | 9.26 | 0.89 | 40.49 | 0.43 | 0.29 | 1.77 | 40.57 | 99.76 |
| | 3.53 | 2.77 | 11.20 | 0.66 | 42.59 | 1.15 | 0.15 | 3.53 | 35.90 | 101.46 |
| | 1.95 | 2.78 | 10.74 | 1.02 | 39.35 | 0.72 | 0.27 | 2.58 | 42.24 | 101.66 |
| Granitic rock* | 0.08 | 0.08 | 8.21 | 86.09 | | 0.76 | 0.06 | 0.04 | 3.35 | 98.67 |

Blank = no data, * = average major element content of granitic rocks at the Rehai geothermal field (Lin *et al.*, 2014).

in volcanic and geothermal settings (Naughton *et al.*, 1976; Aguilera *et al.*, 2016), is discussed here in order to identify the genesis of the sulfate minerals at the Zhenzhu Spring. The main processes in gas condensate alteration include: (1) vapour condensation which causes the acidic gases ($H_2S$ and $SO_2$) to dissolve in the condensate; (2) generation of $H_2SO_4$ in condensates (e.g. oxidation of $H_2S$ and $SO_2$); and (3) interaction between gas condensates and rocks. A general characteristic of the alteration products is the co-occurrence of minerals, such as native sulfur (e.g. Mizutani and Sugiura, 1966; Naughton *et al.*, 1976; Ikehata and Maruoka, 2016) and silica minerals (e.g. cristobalite, tridymite and amorphous $SiO_2$) (McHenry *et al.*, 2017). The gas condensate alteration mechanism is considered as applicable to explain the formation of sulfate minerals around the Zhenzhu Spring.

The sulfur isotope composition is a robust indicator for recognising the origin of sulfate minerals in steam-heated environments because of their relatively small S isotope fractionation during abiotic oxidation of S-bearing minerals (generally $\Delta^{34}S$ (sulfate–sulfide) = $\delta^{34}S$sulfate – $\delta^{34}S$sulfide < 3‰) (Fry *et al.*, 1988; Toran and Harris, 1989; Balci *et al.*, 2007) and sulfate precipitation from fluids (generally $\Delta^{34}S$(sulfate–dissolved $SO_4^{2-}$) < 3‰) (Raab and Spiro, 1991). The $\delta^{34}S$ of dissolved $SO_4^{2-}$ of the spring water and the sulfate samples from the Zhenzhu Spring vary in a way that is consistent with the variation in $\delta^{34}S$ of the $H_2S$ gases, dissolved $SO_4^{2-}$ in other springs and sulfate minerals at the Rehai geothermal field (Fig. 5). This suggests that: (1) the dissolved $SO_4^{2-}$ in the spring waters from the Zhenzhu Spring and others springs at the Rehai geothermal field was contributed mainly by $H_2S$ oxidation; and (2) the sulfur in the sulfate minerals at the Zhenzhu Spring and the sulfate minerals from other areas at the Rehai geothermal field may originate from $H_2S$ oxidation and/or sulfate precipitation of spring water during an evaporation process. At the Zhenzhu Spring, the possibility of the $H_2S$ oxidation mechanism, instead of the sulfate precipitation from spring water, is probable because the spring water cannot inundate the areas where the sulfate minerals were formed.

Because oxygen in sulfate minerals is acquired during oxidation of $H_2S$, the $\delta^{18}O$ of sulfate minerals can provide useful information on their formation. Several factors proposed by Rye *et al.* (1992) are known to be significant in controlling the $\delta^{18}O$ of sulfate minerals in steam-heated environments, including: (1) the ratio of atmospheric oxygen to water oxygen involved in the oxidation of $H_2S$; (2) the oxygen isotope composition of the fluid; and (3) the oxidation temperature and the degree of exchange of oxygen between aqueous sulfate and the fluid. Although low temperature can impede oxygen isotope exchange (Chiba and Sakai, 1985; Holt and Kumar, 1991), oxygen isotope exchange between dissolved $SO_4^{2-}$ and other fluids

https://doi.org/10.1180/mgm.2018.164 Published online by Cambridge University Press

**Table 4.** Sulfur ($\delta^{34}S_{CDT}$) and oxygen ($\delta^{18}O_{VSMOW}$) isotopic analysis data for sulfate minerals, $H_2S$ gases (or pyrite) and spring waters ($SO_4^{2-}$, $H_2O$) from hot springs at the Rehai geothermal field and in some typical steam-heated environments and oxygen isotopic composition of atmospheric $O_2$.

| Location, composition | $\delta^{34}S_{CDT}$ (‰) | $\delta^{18}O_{VSMOW}$ (‰) | References |
|---|---|---|---|
| **Zhenzhu Spring** | | | |
| Gypsum, amorphous $SiO_2$ | 0.77 | −8.94 | This research |
| Gypsum, amorphous $SiO_2$ | −0.33 | −8.49 | This research |
| Gypsum, amorphous $SiO_2$ | 0.51 | −7.79 | This research |
| Gypsum, amorphous $SiO_2$ | 1.69 | −4.60 | This research |
| Gypsum, amorphous $SiO_2$ | 1.88 | −4.62 | This research |
| Al-containing sulfate minerals | 0.98 | 16.48 | This research |
| Al-containing sulfate minerals | −0.05 | 20.10 | This research |
| Al-containing sulfate minerals | 1.47 | 7.78 | This research |
| Al-containing sulfate minerals | 0.94 | 6.71 | This research |
| Al-containing sulfate minerals | 0.96 | 8.93 | This research |
| Al-containing sulfate minerals | 1.30 | 17.90 | This research |
| Al-containing sulfate minerals | 1.19 | 16.84 | This research |
| Spring water ($SO_4^{2-}$) | 0.57 | −4.4 | This research |
| Spring water ($H_2O$) | | −7.2 | Guo *et al.* (2014) |
| Spring water ($H_2O$) | | −8.23 | Zhang *et al.* (2016) |
| **Rehai geothermal field(Not including the Zhenzhu Spring)** | | | |
| Al-containing sulfate minerals | −2.6 to 0.6 | | Tong and Zhang (1989) |
| Spring water ($H_2S$ gas) | −2.9 to 1.8 | | Tong and Zhang (1989) |
| Spring water ($SO_4^{2-}$) | −0.2 to 5.8 | | Tong and Zhang (1989) |
| Spring water ($H_2O$) | | −10.19 to −7.78 | Guo *et al.* (2014) |
| Spring water ($H_2O$) | | −9.8 to −6.7 | Zhang *et al.* (2016) |
| **World** | | | |
| $O_2$ | | 23.88 ± 0.02 | Barkan and Luz (2005) |
| **Solfatara-Pisciarelli volcanic active area** | | | |
| Alunite | −1.08 | 6.19 | Piochi *et al.* (2015) |
| Alunite | 0.26 | 6.08 | Piochi *et al.* (2015) |
| Alunite | 0.41 | 7.28 | Piochi *et al.* (2015) |
| Alunite | −3.35 | 4.21 | Piochi *et al.* (2015) |
| Natroalunite | 2.3 | 8.9 | Cortecci *et al.* (1978) |
| Alunite | 1.2 | 7.9 | Cortecci *et al.* (1978) |
| Alunogen, gypsum | 3.8 | 0.3 | Cortecci *et al.* (1978) |
| Alunogen, gypsum | 3 | 3.3 | Cortecci *et al.* (1978) |
| Alunogen, halotrichite | 0.9 | 4.3 | Cortecci *et al.* (1978) |
| $NH_4$ alumn | 2.1 | 6.6 | Cortecci *et al.* (1978) |
| Unknown* | 2.3 | 5.5 | Cortecci *et al.* (1978) |
| Unknown* | 3.2 | 11.8 | Cortecci *et al.* (1978) |
| $H_2S$ gas | −0.7 to 0.1 | | Mormone *et al.* (2015) |
| Spring water ($H_2O$) | | −5 to 0 | Allard *et al.* (1991) |
| Alunite | 0.9 | −2.3 | Rye *et al.* (1992) |
| **Yellowstone National Park** | | | |
| $H_2S$ gas | −5.5 to 2.6 | | Schoen and Rye, (1970) |
| Spring water ($H_2O$) | | −19.2 to −12.9 | Mckenzie and Truesdell (1977) |
| **Steamboat Springs** | | | |
| Alunite | 0.90 | 7.00 | Rye *et al.* (1992) |
| Pyrite | −2 | | Rye *et al.* (1992) |
| Water ($H_2O$) | | −13.7 to −11.9 | Süer (2004) |
| **Waiotapo geothermal field** | | | |
| Alunite | 7.20 | 15.20 | Rye *et al.* (1992) |
| Pyrite | 3.5 to 7.3 | | Steiner and Rafter (1966) |
| Water ($H_2O$) | | −6.95 to 1.27 | Simmons *et al.* (1994) |

Blank = no data, Unknown* = samples without analysing their mineral composition.

(e.g. meteoric water and magmatic water) at 50–100°C in low-pH fumarolic environments has been observed (Rye, 2005). At the Rehai geothermal field, the low $\delta^{18}O$ of dissolved $SO_4^{2-}$ in the spring water and the subaerial environment of sulfate minerals at the Zhenzhu Spring provide evidence for the weak influence of oxygen isotope exchange between sulfate minerals and spring water on the $\delta^{18}O$ composition of sulfate minerals from the Zhenzhu Spring.

The $\delta^{18}O$ of all sulfate samples from the Zhenzhu Spring falls between the two potential oxygen sources: $H_2O$ (either gas or liquid phase) and $O_2$ (mainly gaseous $O_2$ in atmosphere) (Fig. 5). The high $\delta^{18}O$ of Population 3 shows the majority of sulfate oxygen is derived from atmospheric $O_2$. These sulfate minerals have very high $\delta^{18}O$ values (close to $\delta^{18}O$ of atmospheric $O_2$) and seem to be 'primary sulfates' as proposed by Holt and Kumar (1991). Primary sulfate has also been recorded in 'steam caves' (e.g. Adam and Aburi caves in in the Cerna Valley, Romania) and was considered to be formed during the oxidation process in which abundant atmospheric (and minor atmospheric gaseous $H_2O$) $^{18}O$ exchange occurred (Onac *et al.*, 2011). Sulfate minerals of Population 2 suggest oxidation under less oxic conditions than those of Population 3, indicating that the sulfate oxygen of Population 2 had both atmospheric and $H_2O$ origins (steam, including gaseous and liquid $H_2O$).

https://doi.org/10.1180/mgm.2018.164 Published online by Cambridge University Press

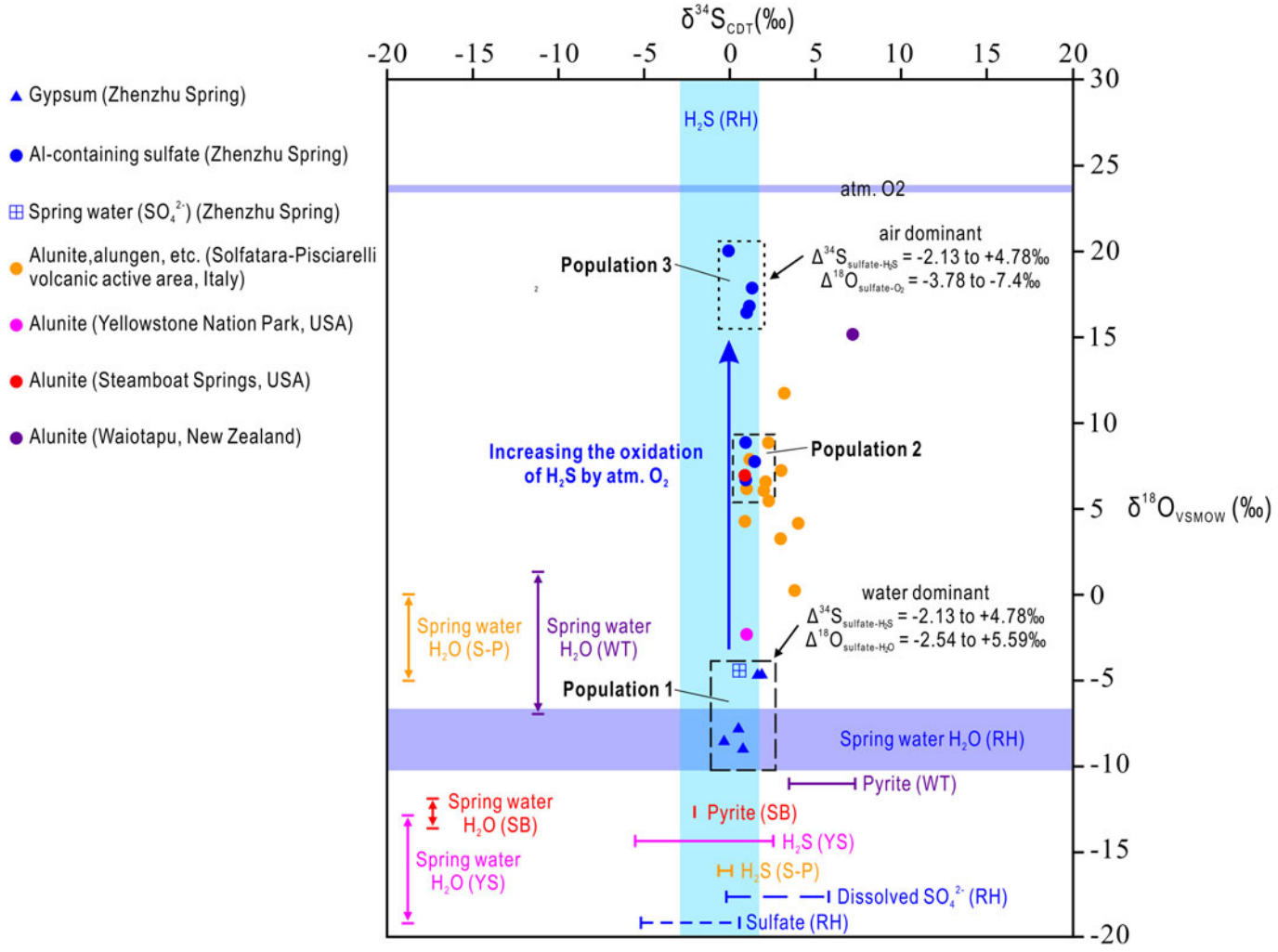


**Fig. 5.** Sulfur ($\delta^{34}S_{CDT}$) and oxygen ($\delta^{18}O_{VSMOW}$) isotope composition for sulfate minerals, $H_2S$ gases and spring water from the Rehai geothermal field, in comparison to potential sources and sulfur-containing minerals (alunite, pyrite and $H_2S$ gas) from other steam-heated environments. RH = Rehai geothermal Field, S-P = Solfatara-Pisciarelli volcanic active area (Italy), YS = Yellowstone National Park (USA), SB = Steamboat Springs (USA), WT = Waiotapu geothermal field (New Zealand) .

The low $\delta^{18}O$ of gypsum from the Zhenzhu Spring may represent: (1) anoxic conditions in which $^{18}O$ can only exchange with $H_2O$; and (2) direct precipitation of gypsum from the fluid in oxic environments. The latter is more reasonable because the areas forming gypsum (i.e. the spring wall) are obviously oxic environments and the fluid precipitating gypsum is the condensed steam. Deposition of the aerosol/steam/fog (tiny water droplets and some vapour) produced by bubble bursting at the water surface forms condensed steam on the rock surface. This process leads the sulfate minerals of Population 3, which are precipitated from the condensed steam, to inherit the O and S isotope composition from spring waters (Fig. 5).

A main source of the metallic elements (Na, Mg, Al, K, Ca and Fe) contained in the sulfate minerals at the Zhenzhu Spring is probably rocks. Although Stoiber and Rose (1974) noted that vapours (gases) from high-temperature (above 330°C) fumarolic vents might contain small concentrations of voltaite cations (i.e. Na, K, Zn, Cu, V and Mo), metallic elements in the sulfate minerals at the Zhenzhu Spring are unlikely to be derived from the vapour because of the relatively low-temperature conditions. The high concentration of Ca in the condensed steam (Table 1) indicates Ca can be derived from the acid aerosols. However, only a few other cations can be transported by the acid aerosols from the Zhenzhu Spring. Under this scenario, rocks appear to be the main source of metallic elements in the formation of sulfate minerals at the Zhenzhu Spring. Acid condensed steams resulting from the precipitation of acid aerosol and condensation of vapour at the Zhenzhu Spring interact with rock debris (e.g. feldspar) and mobilised various elements (e.g. K, Na, Al and Ca) from rocks. Such an important cationic contribution of rocks to the formation of sulfate minerals has also been found in fumarolic environments (Hynek *et al.*, 2013; McCollom *et al.*, 2013) and burning coal-waste heaps (Stracher *et al.*, 2005; Masalehdani *et al.*, 2009).

Collectively, the formation of all the sulfate minerals at the Zhenzhu Spring is controlled by acid aerosols. The following processes are responsible for sulfate mineral formation: (1) formation of underwater water bubbles resulting from intense activity of spring water around vents; (2) water bubble bursting when it arrives at the water surface and forming acid aerosols (composed of tiny water droplets with similar S–O isotope composition to the spring water, and vapour containing $H_2S$); (3) oxidation of $H_2S$ to form $SO_4^{2-}$ with similar $\delta^{34}S$ values to the spring water and different $\delta^{18}O$ values depending on the ratio of air and water oxygen; (4) acid aerosols getting in contact with rocks and forming

https://doi.org/10.1180/mgm.2018.164 Published online by Cambridge University Press

water droplets and/or films; and (5) fluid–rock interaction, releasing various elements and forming sulfate minerals.

### *Comparison with typical modern steam-heated environments*

Rye *et al.* (1992) indicated that most alunites in steam-heated environments (oxidation of $H_2S$) have $\delta^{34}S$ values the same as those of the precursor $H_2S$ (and as related sulfides, if present). This is demonstrated from the $\delta^{34}S$ of alunite and its sulfur origins (pyrite and $H_2S$) from Yellowstone National Park, Steamboat Springs, and Waiotapu geothermal field (Fig. 5). Although no alunite has been found at the Zhenzhu Spring, the $\delta^{34}S$ of the sulfate minerals also falls within the $\delta^{34}S$ range of $H_2S$. This suggests that not only alunite, but also other sulfates (gypsum, alunogen, pickeringite, tamarugite, etc.) in modern steam-heated environments create negligible change in sulfur isotope compositions during their formation processes (oxidation of $H_2S$ and sulfide). Sulfur isotopic exchange between sulfate and $H_2S$/sulfide might occur in steam-heated environments (e.g. Cunningham, 1984; Ebert and Rye, 1997). However, this isotopic exchange process needs a considerable amount time to achieve equilibrium at low temperatures ($4 \times 10^5$ years, if pH = 4 to 7, $T$ = 100°C) (Rye, 2005). In modern steam-heated environments (especially around fumaroles), sulfate minerals may have been formed for only a few years and have not been continuously in contact with the fluid. Thus, the sulfur isotope exchange in modern steam-heated environments is subtle and not significant.

The $\delta^{18}O$ of sulfate minerals from all modern steam-heated environments (except those of Population 1) always reflects the incorporation of atmospheric $O_2$ (Fig. 5). $\Delta^{18}O$(sulfate–$H_2O$) values were found at Yellowstone National Park (10.7 to 16.9‰), Steamboat Springs (18.9 to 20.7.9‰), and Waiotapu (16.47 to 22.5‰), suggesting that the oxidation of $H_2S$/sulfide occurred in a much more oxic environment and no or little $H_2O$ was involved in this process. The $\delta^{18}O$ of sulfate minerals from the Solfatara-Pisciarelli volcanic area varies from 0.3 (close to the $\delta^{18}O$ of the spring water, −5 to 0‰) to 11.8‰. The apparent variation has also been found in the sulfate minerals from the Zhenzhu Spring, and are largely formed by low ratios of atmospheric oxygen to water oxygen. In common with the sulfur isotope data, the $\delta^{18}O$ of sulfate minerals in steam-heated environments can also be influenced by isotopic exchange (Rye *et al.*, 1992; Rye, 2005). However, the oxygen isotopic exchange in modern subaerial environments might not be common because the subaerial condition avoids the contact between sulfate or $SO_4^{2-}$ and fluids.

## Conclusions

Detailed investigations of the samples from the Zhenzhu Spring show that these samples are mainly composed of sulfate minerals (gypsum, alunogen, pickeringite, tamarugite and magnesiovoltaite) and amorphous $SiO_2$. The genesis of the sulfate minerals is related to acid aerosols of tiny water droplets and $H_2S$ vapour. The oxidation of $H_2S$ produces significant amounts of $SO_4^{2-}$ in the aerosol and deposition of this acid aerosol forms the acid condensate on the rocks. The condensate attacks the rocks to form the sulfate minerals with a similar $\delta^{34}S$ value to that of the $H_2S$ and a greater $\delta^{18}O$ value than the spring water. However, some subaerial sulfate minerals with the same $\delta^{18}O$ values as the spring water have been also found and are considered to be the products of the evaporation of some condensed steam (mainly composed of water droplets formed by bubble bursting). This shows that although oxidation of $H_2S$/sulfide plays a key role in the formation of sulfate minerals around acid hot springs, we cannot ignore the $SO_4^{2-}$ derived directly from the acid spring water by bubble bursting. The comparative studies of sulfur-oxygen isotope show that although the $\delta^{34}S$ of the sulfate minerals in modern steam-heated environments displays the same $\delta^{34}S$ values as those of the precursor $H_2S$/sulfide, the $\delta^{18}O$ values of these sulfate minerals are highly variable and influenced largely by the ratio of air and water oxygen. This investigation also suggests that the sulfur or oxygen isotopic exchange between the subaerial sulfate minerals and the fluid might be scarce in some modern steam-heated environments (at least at Zhenzhu Spring).

**Acknowledgements.** Financial support of this study was provided by the National Natural Science Foundation of China (grants 41572097 to Wen and 41472088 to Zheng). The authors wish to thank Yunnan Tengchong Rehai Tour Developing Co. Ltd. for providing permission to sample at Zhenzhu Spring. We also thank Dr. Alejandro Rodríguez and an anonymous reviewer for their constructive and thoughtful comments. The Principal and Production Editors are thanked for copy-editing this manuscript.

## References

Adams P.M., Lynch D.K., Buckland K.N., Johnson P.D. and Tratt D.M. (2017) Sulfate mineralogy of fumaroles in the Salton Sea Geothermal Field, Imperial County, California. *Journal of Volcanology and Geothermal Research*, **347**, 15–43.

Africano F. and Bernard A. (2000) Acid alteration in the fumarolic environment of Usu volcano, Hokkaido, Japan. *Journal of Volcanology and Geothermal Research*, **97**, 475–495.

Aguilera F., Layana S., Rodríguezdíaz A., González C., Cortés J. and Inostroza M. (2016) Hydrothermal alteration, fumarolic deposits and fluids from Lastarria Volcanic Complex: A multidisciplinary study. *Andean Geology*, **43**, 166–196.

Alcicek H., Bulbul A. and Alcicek M.C. (2016) Hydrogeochemistry of the thermal waters from the Yenice Geothermal Field (Denizli Basin, Southwestern Anatolia, Turkey). *Journal of Volcanology and Geothermal Research*, **309**, 118–138.

Allard P., Maiorani A., Tedesco D., Cortecci G. and Turi B. (1991) Isotopic study of the origin of sulfur and carbon in Solfatara fumaroles, Campi Flegrei caldera. *Journal of Volcanology & Geothermal Research*, **48**, 139–159.

Bai D.H., Liao Z.J., Zhao G.Z. and Wang X.B. (1994) The inference of magmatic heat source beneath the Rehai (Hot Sea) field of Tengchong from the result of magnetotelluric sounding. *Chinese Science Bulletin*, **39**, 572–577.

Bai D.H., Meju M.A. and Liao Z.J. (2001) Magnetotelluric images of deep crustal structure of the Rehai geothermal field near Tengchong, southern China. *Geophysical Journal International*, **147**, 677–687.

Balci N., Iii W.C.S., Mayer B. and Mandernack K.W. (2007) Oxygen and sulfur isotope systematics of sulfate produced by bacterial and abiotic oxidation of pyrite. *Geochimica et Cosmochimica Acta*, **71**, 3796–3811.

Barkan E. and Luz B. (2005) High precision measurements of $^{17}O/^{16}O$ and $^{18}O/^{16}O$ ratios in $H_2O$. *Rapid Communications in Mass Spectrometry*, **19**, 3737–3742.

Bonny S. and Jones B. (2003) Microbes and mineral precipitation, Miette Hot Springs, Jasper National Park, Alberta, Canada. *Canadian Journal of Earth Sciences*, **40**, 1483–1500.

Briggs B.R., Brodie E.L., Tom L.M., Dong H.L., Jiang H.C., Huang Q.Y., Wang S., Hou W.G., Wu G., Huang L.Q., Hedlund B.P., Zhang C.L., Dijkstra P. and Hungate B.A. (2014) Seasonal patterns in microbial communities inhabiting the hot springs of Tengchong, Yunnan Province, China. *Environmental Microbiology*, **16**, 1579–1591.

Chiba H. and Sakai H. (1985) Oxygen isotope exchange rate between dissolved sulfate and water at hydrothermal temperatures. *Geochimica et Cosmochimica Acta*, **49**, 993–1000.

https://doi.org/10.1180/mgm.2018.164 Published online by Cambridge University Press

Ciesielczuk J., Zaba J., Bzowska G., Gaidzik K. and Glogowska M. (2013) Sulphate efflorescences at the geyser near Pinchollo, southern Peru. *Journal of South American Earth Sciences*, **42**, 186–193.

Cortecci G., Noto P. and Panichi C. (1978) Environmental isotopic study of the Campi Flegrei (Naples, Italy) geothermal field. *Journal of Hydrology*, **36**, 143–159.

Cunningham C.G. (1984) Origins and exploration significance of replacement and vein-type alunite deposits in the Marysvale volcanic field, west central Utah. *Economic Geology*, **79**, 50–71.

Delines M. (1975) Volcanic sublimates of Rugarama, Kiva region, Republic of Zaire. *Bulletin du Survice Géologique de la Republique du Rwanda*, **8**, 1–11.

Du J.G., Liu C.Q., Fu B.H., Ninomiya Y., Zhang Y.L., Wang C.Y., Wang H.L. and Sun Z.G. (2005) Variations of geothermometry and chemical-isotopic compositions of hot spring fluids in the Rehai geothermal field, southwestern China. *Journal of Volcanology and Geothermal Research*, **142**, 243–261.

Ebert S.W. and Rye R.O. (1997) Secondary precious metal enrichment by steam-heated fluids in the Crofoot-Lewis hot spring gold-silver deposit and relation to paleoclimate. *Economic Geology*, **92**, 578–600.

Fernández-Remolar D.C., Morris R.V., Gruener J.E., Amils R. and Knoll A.H. (2005) The Río Tinto Basin, Spain: mineralogy, sedimentary geobiology, and implications for interpretation of outcrop rocks at Meridiani Planum, Mars. *Earth and Planetary Science Letters*, **240**, 149–167.

Fry B., Ruf W., Gest H. and Hayes J. (1988) Sulfur isotope effects associated with oxidation of sulfide by $O_2$ in aqueous solution. *Chemical Geology: Isotope Geoscience Section*, **73**, 205.

Guo Q.H. (2012) Hydrogeochemistry of high-temperature geothermal systems in China: A review. *Applied Geochemistry*, **27**, 1887–1898.

Guo Q.H. and Wang Y.X. (2012) Geochemistry of hot springs in the Tengchong hydrothermal areas, Southwestern China. *Journal of Volcanology & Geothermal Research*, **215–216**, 61–73.

Guo Q.H., Liu M.L., Li J.X., Zhang X.B. and Wang Y.X. (2014) Acid hot springs discharged from the Rehai hydrothermal system of the Tengchong volcanic area (China): formed via magmatic fluid absorption or geothermal steam heating? *Bulletin of Volcanology*, **76**, 868–879.

Holt B.D. and Kumar R. (1991) Oxygen isotope fractionation for understanding the sulphur cycle. Pp. 27–41 in: *Stable Isotopes: Natural and Anthropogenic Sulphur in the Environment* (H.R. Krouse and V.A. Grinenko, editors). Wiley & Sons, New York.

Hong L., Zhang G.P., Jin Z.S., Liu C.Q., Han G.L. and Ling L.I. (2009) Geochemical characteristics of geothermal fluid in Tengchong Area, Yunnan Province,China. *Acta Mineralogica Sinica*, **29**, 496–501 [in Chinese with English Abstract].

Hou W.G., Wang S., Dong H.L., Jiang H.C., Briggs B.R., Peacock J.P., Huang Q.Y., Huang L.Q., Wu G., Zhi X.Y., Li W.J., Dodsworth J.A., Hedlund B.P., Zhang C.L., Hartnett H.E., Dijkstra P. and Hungate B.A. (2013) A comprehensive census of microbial diversity in hot springs of Tengchong, Yunnan Province China using 16S rRNA gene pyrosequencing. *PLoS One*, **8**, e53350.

Huang X.W., Zhou M.F., Wang C.Y., Robinson P.T., Zhao J.H. and Qi L. (2013) Chalcophile element constraints on magma differentiation of Quaternary volcanoes in Tengchong, SW China. *Journal of Asian Earth Sciences*, **76**, 1–11.

Hynek B.M., McCollom T.M., Marcucci E.C., Brugman K. and Rogers K.L. (2013) Assessment of environmental controls on acid-sulfate alteration at active volcanoes in Nicaragua: Applications to relic hydrothermal systems on Mars. *Journal of Geophysical Research: Planets*, **118**, 2083–2104.

Ikehata K. and Maruoka T. (2016) Sulfur isotopic characteristics of volcanic products from the September 2014 Mount Ontake eruption, Japan. *Earth Planets and Space*, **68**, 1–7.

Jiang C.S. (1998) Period division of volcano activities in the Cenozoic era of Tengchong. *Journal of Seismological Research*, **21**, 320–329 [in Chinese with English Abstract].

Jiang M., Tan H.D., Zhang J.W., Peng M., Li Q.Q., Zhang L.H., Xu L.H. and Wang W. (2012) Geophysical mode of Mazhan-Gudong magma chamber in Tengchong volcano-tectonic area. *Acta Geoscientica Sinica*, **33**, 731–739 [in Chinese with English Abstract].

Jiang Z., Li P., Tu J., Wei D.Z., Zhang R., Wang Y.H. and Dai X.Y. (2018) Arsenic in geothermal systems of Tengchong, China: Potential contamination on freshwater resources. *International Biodeterioration & Biodegradation*, **128**, 28–35.

Jones B. and Peng X.T. (2015) Laminae development in opal-A precipitates associated with seasonal growth of the form-genus Calothrix (Cyanobacteria), Rehai geothermal area, Tengchong, Yunnan Province, China. *Sedimentary Geology*, **319**, 52–68.

Kodosky L. and Keskinen M. (1990) Fumarole distribution, morphology, and encrustation mineralogy associated with the 1986 eruptive deposits of mount St. *Augustine, Alaska.* Bulletin of Volcanology, **52**, 175–185.

Liao Z.J., Shen M.Z. and Guo G.Y. (1991) Characteristics of the Reservoir of the Rehai Geothermal Field in Tengchong, Yunnan Province, China. *Acta Geologica Sinica (English Edition)*, **4**, 307–320.

Lin M.S., Peng S.B., Qiao W.T. and Li H. (2014) Petro-geochemistry and geochronology of late Cretaceous-Eocene granites in high geothermal anomaly areas in the Tengchong block, Yunnan Province, China and their tectonic implications. *Acta Petrologica Sinica*, **30**, 527–546 [in Chinese with English Abstract].

Liu L., Salam N., Jiao J.Y., Jiang H.C., Zhou E.M., Yin Y.R., Ming H. and Li W.J. (2016) Diversity of culturable thermophilic actinobacteria in hot springs in Tengchong, China and studies of their biosynthetic gene profiles. *Microbial Ecology*, **72**, 150–162.

Martin R., Rodgers K. and Browne P. (1999) The nature and significance of sulphate-rich, aluminous efflorescences from the Te Kopia geothermal field, Taupo Volcanic Zone, New Zealand. *Mineralogical Magazine*, **63**, 413–413.

Masalehdani M.N.-N., Mees F., Dubois M., Coquinot Y., Potdevin J.-L., Fialin M. and Blanc-Valleron M.-M. (2009) Condensate minerals from a burning coal-waste heap in Avion, Northern France. *The Canadian Mineralogist*, **47**, 573–591.

McCollom T.M., Hynek B.M., Rogers K., Moskowitz B. and Berquo T.S. (2013) Chemical and mineralogical trends during acid-sulfate alteration of pyroclastic basalt at Cerro Negro volcano and implications for early Mars. *Journal of Geophysical Research-Planets*, **118**, 1719–1751.

McHenry L.J., Carson G.L., Dixon D.T. and Vickery C.L. (2017) Secondary minerals associated with Lassen fumaroles and hot springs: Implications for Martian hydrothermal deposits. *American Mineralogist*, **102**, 1418–1434.

Mckenzie W.F. and Truesdell A.H. (1977) Geothermal reservoir temperatures estimated from the oxygen isotope compositions of dissolved sulfate and water from hot springs and shallow drillholes. *Geothermics*, **5**, 51–61.

Mizutani Y. and Sugiura T. (1966) The chemical equilibrium of the $2H_2S + SO_2 = 3S + 2H_2O$ reaction in solfataras of the Nasudake Volcano. *Bulletin of the Chemical Society of Japan*, **39**, 2411–2414.

Mormone A., Troise C., Piochi M., Balassone G., Joachimski M. and Natale G.D. (2015) Mineralogical, geochemical and isotopic features of tuffs from the CFDDP drill hole: Hydrothermal activity in the eastern side of the Campi Flegrei volcano (southern Italy). *Journal of Volcanology & Geothermal Research*, **290**, 39–52.

Naughton J.J., Greenberg V.A. and Goguel R. (1976) Incrustations and fumarolic condensates at Kilauea volcano, Hawaii: field, drill-hole and laboratory observations. *Journal of Volcanology and Geothermal Research*, **1**, 149–165.

Onac B.P., Wynn J.G. and Sumrall J.B. (2011) Tracing the sources of cave sulfates: a unique case from Cerna Valley, Romania. *Chemical Geology*, **288**, 105–114.

Pierre D. and Alain B. (1994) Geochemistry, mineralogy, and chemical modeling of the acid crater lake of Kawah Ijen Volcano, Indonesia. *Geochimica et Cosmochimica Acta*, **58**, 2445–2460.

Piochi M., Mormone A., Balassone G., Strauss H., Troise C. and De Natale G. (2015) Native sulfur, sulfates and sulfides from the active Campi Flegrei volcano (southern Italy): Genetic environments and degassing dynamics revealed by mineralogy and isotope geochemistry. *Journal of Volcanology and Geothermal Research*, **304**, 180–193.

Raab M. and Spiro B. (1991) Sulfur isotopic variations during seawater evaporation with fractional crystallization. *Chemical Geology Isotope Geoscience*, **86**, 323–333.

Rodgers K.A., Hamlin K.A., Browne P.R.L., Campbell K.A. and Martin R. (2000) The steam condensate alteration mineralogy of Ruatapu cave, Orakei Korako geothermal field, Taupo Volcanic Zone, New Zealand. *Mineralogical Magazine*, **64**, 125–142.

Rodríguez A. and van Bergen M.J. (2016) Volcanic hydrothermal systems as potential analogues of Martian sulphate-rich terrains. *Netherlands Journal of Geosciences*, **95**, 153–169.

https://doi.org/10.1180/mgm.2018.164 Published online by Cambridge University Press

Rodríguez A. and van Bergen M.J. (2017) Superficial alteration mineralogy in active volcanic systems: An example of Poás volcano, Costa Rica. *Journal of Volcanology and Geothermal Research*, **346**, 54–80.

Rye R.O. (2005) A review of the stable-isotope geochemistry of sulfate minerals in selected igneous environments and related hydrothermal systems. *Chemical Geology*, **215**, 5–36.

Rye R.O., Bethke P.M. and Wasserman M.D. (1992) The stable isotope geochemistry of acid sulfate alteration. *Economic Geology*, **87**, 225–262.

Sakae T., Okada S., Okamura K. and Nakano K. (2011) Unique form hot spring sinter composed of gypsum with special reference to the relation between microorganisms and mineralization. *Journal of Hard Tissue Biology*, **20**, 339–343 [in Japanese with English Abstract].

Schiffman P., Zierenberg R., Marks N., Bishop J.L. and Dyar M.D. (2006) Acid-fog deposition at Kilauea volcano: A possible mechanism for the formation of siliceous-sulfate rock coatings on Mars. *Geology*, **34**, 921–924.

Schoen R. and Rye R.O. (1970) Sulfur isotope distribution in Solfataras, Yellowstone National Park. *Science*, **170**, 1082–1084.

Shangguan Z.G. (2000) Structure of geothermal reservoirs and the temperature of mantle-derived magma hot source in the Rehai area, Tengchong. *Acta Petrologica Sinica*, **16**, 83–90 [in Chinese with English Abstract].

Shangguan Z.G. and Huo W.G. (2002) delta D values of escaped $H_2$ from hot springs at the Tengchong Rehai geothermal area and its origin. *Chinese Science Bulletin*, **47**, 146–149.

Shangguan Z.G., Bai C.H. and Sun M.L. (2000) Mantle-derived magmatic gas releasing features at the Rehai area, Tengchong county, Yunnan Province, China. *Science in China Series D-Earth Sciences*, **43**, 132–140.

Simmons S.F., Stewart M.K., Robinson B.W. and Glover R.B. (1994) The chemical and isotopic compositions of thermal waters at Waimangu, New Zealand. *Geothermics*, **23**, 539–553.

Steiner A. and Rafter T.A. (1966) Sulfur isotopes in pyrite, pyrrhotite, alunite and anhydrite from steam wells in the Taupo Volcanic Zone, New Zealand. *Economic Geology*, **61**, 1115–1129.

Stoiber R.E. and Rose W.I. (1974) Fumarole incrustations at active Central American volcanoes. *Geochimica et Cosmochimica Acta*, **38**, 495–516.

Stracher G.B., Prakash A., Schroeder P., McCormack J., Zhang X.M., Van Dijk P. and Blake D. (2005) New mineral occurrences and mineralization processes: Wuda coal-fire gas vents of Inner Mongolia. *American Mineralogist*, **90**, 1729–1739.

Süer S. (2004) *Monitoring of Chemical and Isotopic Compositions of Geothermal Waters along the North Anatolian Fault Zone*. Master Thesis. Middle East Technical University, Turkey.

Szynkiewicz A., Modelska M., Buczyński S., Borrok D.M. and Merrison J.P. (2013) The polar sulfur cycle in the Werenskioldbreen, Spitsbergen: Possible implications for understanding the deposition of sulfate minerals in the North Polar Region of Mars. *Geochimica et Cosmochimica Acta*, **106**, 326–343.

Tang M., Ehreiser A. and Li Y.L. (2014) Gypsum in modern Kamchatka volcanic hot springs and the Lower Cambrian black shale: Applied to the microbial-mediated precipitation of sulfates on Mars. *American Mineralogist*, **99**, 2126–2137.

Tong W. and Zhang M.Z. (1989) *Geothermics in Tengchong*. Science Press, Beijing [in Chinese].

Toran L. and Harris R.F. (1989) Interpretation of sulfur and oxygen isotopes in biological and abiological sulfide oxidation. *Geochimica et Cosmochimica Acta*, **53**, 2341–2348.

Valente T.M. and Gomes C.L. (2009) Occurrence, properties and pollution potential of environmental minerals in acid mine drainage. *Science of the Total Environment*, **407**, 1135–1152.

Wang C. and Gang H. (2004) Crustal structure in Tengchong Volcano-Geothennal Area, western Yunnan, China. *Tectonophysics*, **380**, 69–87.

White W.B. (2010) Secondary minerals in volcanic caves: Data from Hawai'i. *Journal of Cave and Karst Studies*, **72**, 75–85.

Xu Y., Yang X.T., Li Z.W. and Liu J.H. (2012) Seismic structure of the Tengchong volcanic area southwest China from local earthquake tomography. *Journal of Volcanology and Geothermal Research*, **239–240**, 83–91.

Yang H.Y., Hu J.F., Hu Y.L., Duan Y.Z. and Li G.Q. (2013) Crustal structure in the Tengchong volcanic area and position of the magma chambers. *Journal of Asian Earth Sciences*, **73**, 48–56.

Zhang G.P., Liu C.Q., Liu H., Jin Z.S. and Han G.L. (2008) Geochemistry of the Rehai and Ruidian geothermal waters, Yunnan Province, China. *Geothermics*, **37**, 73–83.

Zhang Y.F., Tan H.B., Zhang W.J., Wei H.Z. and Dong T. (2016) Geochemical constraint on origin and evolution of solutes in geothermal springs in western Yunnan, China. *Chemie der Erde – Geochemistry*, **76**, 63–75.

Zhao C.P., Ran H. and Chen K.H. (2011) Present-day temperatures of magma chambers in the crust beneath Tengchong volcanic field, southwestern China: Estimation from carbon isotopic fractionation between $CO_2$ and $CH_4$ of free gases escaped from thermal springs. *Acta Petrologica Sinica*, **27**, 2883–2897 [in Chinese with English Abstract].

Zhu M.X., Tong W. and You M.Z. (1980) Efflorescence in geothermal areas of Xizang (Tibet) and its geological significance. *Acta Scientiarum Naturalum Universitis Pekinensis*, 110–117 [in Chinese with English Abstract].

Zou H.B., Fan Q.C., Schmitt A.K. and Sui J.L. (2010) U-Th dating of zircons from Holocene potassic andesites (Maanshan volcano, Tengchong, SE Tibetan Plateau) by depth profiling: Time scales and nature of magma storage. *Lithos*, **118**, 202–210.

https://doi.org/10.1180/mgm.2018.164 Published online by Cambridge University Press